Journal of Experimental Nanoscience
Publication details, including instructions for authors and subscription information:
http://www.informaworld.com/smpp/title~content=t716100757

Small angle X-ray scattering and photoluminescence study of ZnO nanoparticles synthesized by hydrothermal process

Raghvendra S. Yadav[a]; Avinash C. Pandey[a]
[a] Nanophosphor Application Centre, University Of Allahabad, Allahabad-211002, India

To cite this Article Yadav, Raghvendra S. and Pandey, Avinash C.(2007) 'Small angle X-ray scattering and photoluminescence study of ZnO nanoparticles synthesized by hydrothermal process', Journal of Experimental Nanoscience, 2: 3, 177 — 182
To link to this Article: DOI: 10.1080/17458080701474242
URL: http://dx.doi.org/10.1080/17458080701474242

Journal of Experimental Nanoscience,
Vol. 2, No. 3, September 2007, 177–182

Taylor & Francis
Taylor & Francis Group

Small angle X-ray scattering and photoluminescence study of ZnO nanoparticles synthesized by hydrothermal process

RAGHVENDRA S. YADAV* and AVINASH C. PANDEY

Nanophosphor Application Centre, University Of Allahabad, Allahabad-211002, India

(*Received March 2007; in final form May 2007*)

Polydisperse ZnO nanoparticles have been synthesized by a hydrothermal process. Small-angle X-ray Scattering (SAXS) was performed for particle size distribution analysis of ZnO nanoparticles. Room-temperature photoluminescence measurements revealed that the ZnO nanoparticles have a single visible emission peak ~600 nm, although polydispersity of the sample shows no presence on PL spectrum. It seems the orange emission ~600 nm is due to the presence of $Zn(OH)_2$ on the surface of ZnO nanoparticles, instead of the commonly assumed interstitial oxygen defect.

Keywords: ZnO; Photoluminescence; Hydrothermal process; SAXS

1. Introduction

Zinc oxide (ZnO) is a wurtzitic semiconductor with a direct band gap of 3.37 eV at room temperature [1]. Due to the large-band-gap energy, ZnO becomes an excellent semiconductor material for applications considered for other wide-band-gap materials such as GaN and SiC. In addition to this, due to the extremely large exciton binding energy (about 60 meV) [2, 3], the excitons in ZnO are thermally stable at room temperature, and thus, ZnO has significant advantages in optoelectronic applications. Although ZnO's luminescence has been the subject of studies for several decades, the centers and mechanisms responsible for many of its luminescence properties are still a matter of controversy. ZnO typically exhibits UV band edge emission and a broad visible band due to defect emission [4, 5]. It is noted that different types of defects are responsible for violet, blue, green, yellow and orange-red emissions in ZnO, but the chemical nature of the defects responsible for the orange emission is less reported. It was also reported that the size [6], the surface of nanoparticle [7–9] and fabrication method [10] have an effect on the luminescence properties. A number of different hypotheses have been proposed to explain the orange emission in ZnO.

*Corresponding author. Email: raghvendra_nac@yahoo.co.in

Journal of Experimental Nanoscience
ISSN 1745–8080 print/ISSN 1745–8099 online © 2007 Taylor & Francis
http://www.tandf.co.uk/journals
DOI: 10.1080/17458080701474242

The yellow-orange defect emission observed in ZnO synthesized by a hydrothermal method is typically assigned to an interstitial oxygen [11, 12], although other hypotheses such as dislocation related luminescence centers [13] and Li dopants [14] have been proposed. The green emission is typically associated with oxygen deficiency, yellow/orange emission is associated with excess oxygen [15]. In this article, we show the orange luminescence (~600 nm) in ZnO nanoparticles synthesized by the hydrothermal process, due to the presence of hydroxyl groups on the surface of ZnO nanoparticles.

2. Experimental section

2.1. *Chemical*

The zinc acetate dihydrate (98%) $Zn(CH_3COO)_2 \cdot 2H_2O$, sodium hydroxide NaOH were from E. Merck Limited, Mumbai-400018, India. These chemicals were directly used without special treatment.

2.2. *Sample preparation*

In a typical hydrothermal synthesis process: 1 g of zinc acetate dihydrate was put into 110 mL of double distilled water under vigorous stirring. After 10 min stirring, 10 mL of 2M NaOH aqueous solution was introduced into the above aqueous solution, resulting in a white aqueous solution for which the pH value was maintained at 12. Then the prepared solution was transferred into a stainless steel autoclave, sealed and maintained at the temperature of 110°C for 4 h. The resulting white solid products were centrifuged, washed with distilled water and ethanol to remove any ions possibly remaining in the final products, and finally dried at 60°C in air.

2.3. *Apparatus*

Particle size distribution of the obtained ZnO nanoparticles were characterized by small-angle X-ray scattering, carried out on a Rigaku D/MAX-2200H/PC using Cu Kα radiation ($\lambda = 1.54056$ Å).The transmission electron microscopy (TEM) images were taken on a Philips CM 12 microscope operated at 110 kV. The photoluminescence was studied by 325 nm radiation from He–Cd laser (KIMMON) and Mechelle 900 spectrograph.

3. Result and discussion

3.1. *The morphology of product*

The morphology of ZnO nanoparticles were investigated by transmission electron microscopy (Philips CM 12). Figure 1 shows the TEM image of ZnO nanoparticles synthesized by hydrothermal process. Figure 1 confirmed the formation of spherical-like ZnO nanoparticles. It is also clear that in the hydrothermal synthesis of ZnO

nanoparticles there is less, not more, agglomeration between the ZnO nanoparticles, which is a disadvantage of the hydrothermal process. Therefore, due to the small amount of agglomeration between some ZnO nanoparticles, accurate measurement of particle size distribution from the TEM study was not possible in an easy manner. So a small-angle X-ray scattering study was carried out.

3.2. *Particle size distribution from SAXS study*

Figure 2 shows the small-angle X-ray scattering pattern from ZnO nanoparticles. The scattering intensity I (s) from the ZnO nanoparticles follows the Guinier

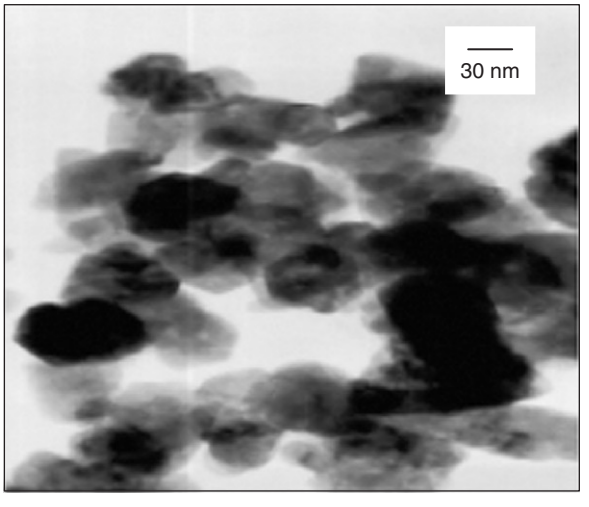

Figure 1. TEM image of spherical-like ZnO nanoparticle synthesized by hydrothermal process.

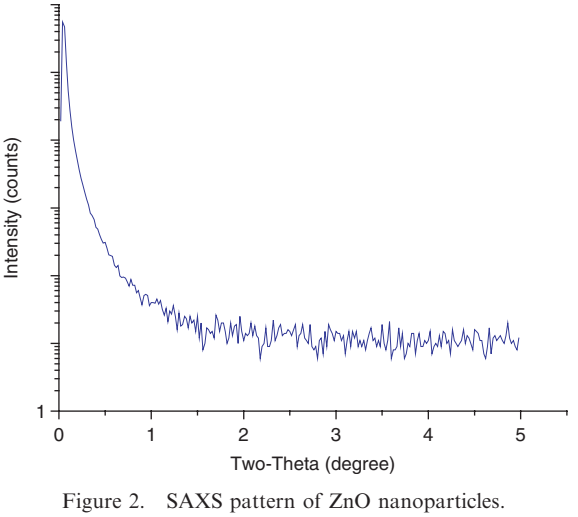

Figure 2. SAXS pattern of ZnO nanoparticles.

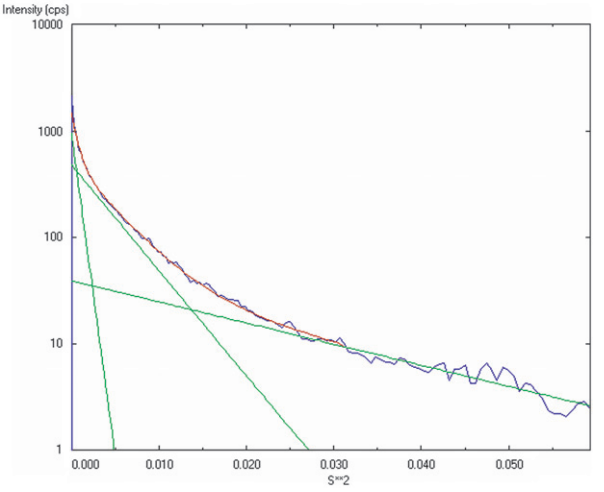

Figure 3. Guinier plot of scattered intensity from ZnO nanoparticles.

small-angle scattering intensity equation [16]:

$$I(s) = I_e \cdot M \cdot n^2 \cdot \exp(s^2 \cdot R_0/3)$$

Here I_e, M, n, s and R_0 are scattering intensity per electron, the number of grain, the number of electrons per grain, scattering vector and inertial radius respectively. The particle size distributions of the ZnO nanoparticles could be calculated by simply plotting tangents on the curve of the graph $\log I - s^2$ (Fankuchen Method) [17]. Figure 3 shows a Guinier plot of scattered intensity from the ZnO nanoparticles. The Guinier plot of the scattered intensity from ZnO nanoparticles indicated that there is the formation of polydisperse ZnO nanoparticles by hydrothermal process. Particle size distribution of ZnO nanoparticles by analysis of Guinier plot of scattered intensity is 28.7 wt% particles of 24 nm size, 29.7 wt% particles of 12 nm and 41.6 wt% of 7 nm. This particle size distribution calculation was done by grain size analysis program provided by Rigaku D/Max-2200 H/PC.

4. Optical study

Figure 4 illustrates the photoluminescence spectrum of ZnO nanoparticles under photon excitation of 325 nm. Room-temperature photoluminescence revealed that the ZnO nanoparticles have an orange visible emission band at ~600 nm, whereas no UV band ~384 nm was observed. The orange emission in samples prepared by a hydrothermal method is due to the presence of $Zn(OH)_2$ on the surface of ZnO nanoparticles instead of the commonly assumed interstitial oxygen defect [18], and the quenching of excitonic transition of ZnO nanoparticles is also due to the presence of $Zn(OH)_2$ on the surface of ZnO nanoparticles [19]. The ZnO sample consists of

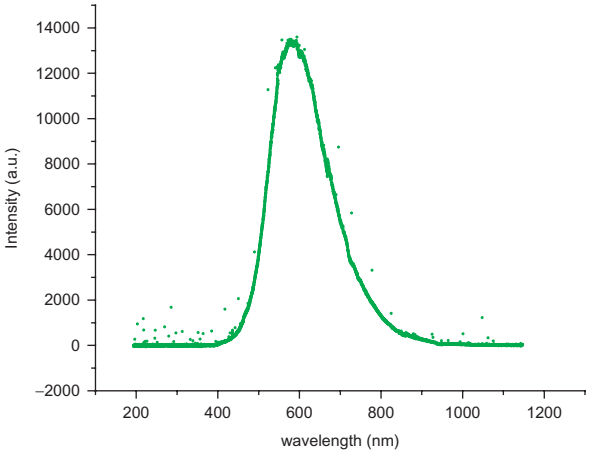

Figure 4. Room temperature PL spectrum of ZnO nanoparticles synthesized by hydrothermal process.

nanoparticles of different sizes such as 28.7% of 24 nm, 29.7% of 12 nm and 41.6% of 7 nm; but no significant size effect are observed in PL spectrum. Therefore, the luminescence properties are due to the possible presence of $Zn(OH)_2$ at the surface of ZnO nanoparticles. This explanation for orange visible emission and no UV band is seeming reasonable for the sample synthesized by hydrothermal method, since there is the possible presence of hydroxyl groups on surface of ZnO nanoparticles synthesized by the hydrothermal method instead of others.

To summarize, we have investigated the particle size of ZnO nanoparticles by SAXS study. From the SAXS study, it is clear that hydrothermally synthesized ZnO nanoparticles are polydispersed. These ZnO nanoparticles are of different sizes viz. 28.7% of 24 nm, 29.7% of 12 nm and 41.6% of 7 nm. There is no size-dependent emission peak in PL spectrum of ZnO nanoparticles. The orange emission and quenching of excitonic transition in the sample is due to presence of $Zn(OH)_2$ on surface of ZnO nanoparticles, instead of the commonly assumed interstitial oxygen defect.

Acknowledgements

We acknowledge the support obtained from various institutions like IUAC (Delhi) with special thanks to Mr. Manavendra Kumar for PL measurement, Banaras Hindu University (Varanasi) for TEM measurement.

References

[1] Y.F. Chen, D.M. Bagnall, H. Koh, K. Park, K. Hiraga, Z. Zhu, T. Yao. Plasma assisted molecular beam epitaxy of ZnO on c-plane sapphire: growth and characterization. *J. Appl. Phys.*, **84**, 3912 (1998).
[2] W.Y. Liang, A.D. Yoffe. Transmission spectra of ZnO single crystals. *Phys. Rev. Lett.*, **20**, 59 (1968).
[3] D.C. Reynolds, D.C. Look, B. Jogai, C.W. Litton, G. Cantwell, W.C. Harsch. Valence-band ordering in ZnO. *Phys. Rev. B*, **60**, 2340 (1999).
[4] U. Özgür, Ya I. Alivov, C. Liu, A. Teke, M.A. Reshchikov, S. Doğan, V. Avrutin, S.-J. Cho, H. Morkoç. A comprehensive review of ZnO materials and devices. *J. Appl. Phys.*, **98**, 041301 (2005).

[5] A.B. Djurišić, Y.H. Leung. Optical properties of ZnO nanostructures. *Small*, **2**, 944 (2006).
[6] A. Van Dijken, E.A. Meukenkamp, D. Vanmaekelbergh, A. Meijerink. The luminescence of nanocrystalline ZnO particles: the mechanism of the ultraviolet and visible emission. *J. Lumin.*, **87**, 454 (2000).
[7] L. Guo, S. Yang, C. Yang, P. Yu, J. Wang, W. Ge, G.K.L. Wong. Highly monodisperse polymer-capped ZnO nanoparticles: preparation and optical properties. *Appl. Phys. Lett.*, **76**, 2901 (2000).
[8] S. Mahamuni, K. Borgohain, B.S. Bendre, V. Leppert, S.H. Risbud. Spectroscopic and structural characterization of electrochemically grown ZnO quantum dots. *J. Appl. Phys.*, **85**, 2861 (1999).
[9] K. Borgohain, S. Mahamuni. Luminescence behaviour of chemically grown ZnO quantum dots. *Semicond. Sci. Technol.*, **13**, 1154 (1998).
[10] D. Li, Y.H. Leung, A.B. Djurišić, Z.T. Liu, M.H. Xie, S.L. Shi, S.J. Xu, W.K. Chan. Different origins of visible luminescence in ZnO nanostructures fabricated by the chemical and evaporation methods. *Appl. Phys. Lett.*, **85**, 1601 (2004).
[11] W.M. Kwok, A.B. Djurišić, Y.H. Leung, W.K. Chan, D.L. Phillips. Time-resolved photoluminescence study of the stimulated emission in ZnO nanoneedles. *Appl. Phys. Lett.*, **87**, 093108 (2005).
[12] L.E. Greene, M. Law, J. Goldberger, F. Kim, J.C. Johnson, Y. Zhang, R.J. Saykally, P. Yang. Low-temperature wafer-scale production of ZnO nanowire arrays. *Angew. Chem. Int. Ed.*, **42**, 3031 (2003).
[13] R. Radoi, P. Fernández, J. Piqueras, M.S. Wiggins, J. Solis. Luminescence properties of mechanically milled and laser irradiated ZnO. *Nanotechnology*, **14**, 794 (2003).
[14] N. Ohashi, N. Ebisawa, T. Sekiguchi, I. Sakaguchi, Y. Wada, T. Takenaka, H. Haneda. Yellowish-white luminescence in codoped zinc oxide. *Appl. Phys. Lett.*, **86**, 091902 (2005).
[15] S.A. Studenikin, N. Golego, M. Cocivera. Fabrication of green and orange photoluminescent undoped ZnO films using spray pyrolysis. *J. Appl. Phys.*, **84**, 2287 (1998).
[16] A. Guinier, G. Fournet. *Small-angle of X-ray*, John Wiley & Sons, New York (1955).
[17] E. Alexander Leroy. *X-ray Diffraction Methods in Polymer Science*, John Wiley & Sons, New York (1969).
[18] A.B. Djurišić, Y.H. Leung, K.H. Tam, Y.F. Hsu, L. Ding, W.K. Ge, Y.C. Zhong, K.S. Wong, W.K. Wong, W.K. Chan, H.L. Tam, K.W. Cheah, W.M. Kwok, D.L. Phillips. Defect emissions in ZnO nanostructures. *Nanotechnology*, **18**, 095702 (2007).
[19] H. Zhou, H. Alves, D.M. Hofmann, W. Kriegseis, B.K. Meyer, G. Kaczmarczyk, A. Hoffmann. Behind the weak excitonic emission of ZnO quantum dots:ZnO/$Zn(OH)_2$ core-shell structure. *Appl. Phys. Lett.*, **80**, 210 (2002).